

Article

Study on Temporal and Spatial Variation in Soil Temperature in Artificial Ground Freezing of Subway Cross Passage

Baoping Zou ¹, Bo Hu ¹, Jianzhong Xia ¹, Xiaoquan Li ², Qizhi Chen ^{1,*}, Bowen Kong ¹ and Jingyuan Ma ¹

¹ School of Civil Engineering and Architecture, Zhejiang University of Science & Technology, Hangzhou 310023, China

² School of Architecture and Engineering, Zhejiang Guangsha Vocational and Technical University of Construction, Dongyang 322100, China

* Correspondence: chenqizhi@zust.edu.cn

Abstract: Temperature is the fundamental variable used in artificial ground freezing (AGF) design to assess the frozen curtain's state and carry out an analysis of its mechanical behavior. Therefore, it is important to appropriately understand the temperature variation in the soil during freezing and thawing throughout the construction process of AGF. In this paper, a soil physical state analysis model was established to obtain the one-dimensional distribution curve of the soil temperature field and the temperature variation curve of the soil with temporal, which can be used to explore the soil temperature characteristics during the construction of AGF, so as to scientifically evaluate the physical state of frozen soil and reduce the construction risk. The soil can be divided into three zones during the construction process of AGF, namely the frozen zone, the frozen fringe, and the unfrozen zone. Additionally, Hangzhou muddy silty clay was selected for the indoor model test to verify the correctness of the analytical model. The results show the following: (1) Due to the influence of the latent heat of the phase change, the physical state and temperature of the soil on both sides of the frozen fringe are not the same. It is not appropriate to use the same temperature index to judge whether the soil is frozen or thawed in the project. (2) For Hangzhou muddy silty clay, the freezing index is $-1\text{ }^{\circ}\text{C}$, and the thawing index is $0.9\text{ }^{\circ}\text{C}$. The research results can provide some guidance for the judgment of the soil state during the AGF of subway cross passages.

Keywords: artificial ground freezing (AGF); subway cross passage; soil physical state analysis model; indoor test; temporal and spatial variation in temperature



check for updates

Citation: Zou, B.; Hu, B.; Xia, J.; Li, X.; Chen, Q.; Kong, B.; Ma, J. Study on Temporal and Spatial Variation in Soil Temperature in Artificial Ground Freezing of Subway Cross Passage. *Sustainability* **2023**, *15*, 3663. <https://doi.org/10.3390/su15043663>

Academic Editors: Mingfeng Lei, Jianjun Ma, Yu Liang and Yuexiang Lin

Received: 23 January 2023

Revised: 14 February 2023

Accepted: 14 February 2023

Published: 16 February 2023



Copyright: © 2023 by the authors. Licensee MDPI, Basel, Switzerland. This article is an open access article distributed under the terms and conditions of the Creative Commons Attribution (CC BY) license (<https://creativecommons.org/licenses/by/4.0/>).

1. Introduction

Urban congestion is becoming increasingly prevalent with rapid economic development. To alleviate this phenomenon, the development and utilization of urban underground space are becoming more and more important. Subways, as an underground transportation mode, occupy an important position in the process of underground space development and utilization [1]. In subway tunnel construction, cross passages with fire prevention, drainage, and connection functions should be set up at specific intervals [2,3]. However, when the project is located in a soft soil area, due to the low soil bearing capacity and high water content, engineering disasters such as hole collapses and ground settlement during the excavation process may be caused; it is necessary to strengthen the soil layer before construction [4–7]. Artificial ground freezing (AGF) is a green technology that, in keeping with the concept of sustainable development, uses freezing technology to turn the natural layer into an artificially frozen layer. It is currently commonly utilized for soil reinforcement in subway cross passages in soft soil areas [8–11].

The temperature has a direct influence on the strength and thickness of the frozen soil curtain; therefore, the soil temperature is generally used to judge the physical state of the soil in practical engineering [12–14]. In order to understand the distribution of the

soil temperature field during the construction process of AGF, researchers have conducted extensive research on this issue either based on field monitoring data or finite element software [15–19]. The AGF construction process is characterized by complex environmental factors such as groundwater seepage, freezing pipe placement, and initial ground temperature, all of which have an impact on the soil temperature field. The seepage of groundwater can alter the cooling capacity provided by the refrigeration tubes and affect the soil temperature [20,21]. Zhou et al. [22] established a model for the freezing method of a composite stratum seepage environment based on indoor tests, and explored the influence of seepage on the freezing method's construction and surrounding engineering environment; Xu et al. [23] established a numerical model of the coupling of the seepage field and the temperature field in a cross passage to simulate the influence of the groundwater velocity, freezing pipe diameter, initial ground temperature, and freezing pipe spacing on the temperature field development under single-row freezing. The results show that the influence of the four factors on the freezing temperature field in descending order is groundwater flow rate, freezing pipe spacing, freezing pipe diameter, and initial ground temperature; Qin et al. [24] found that groundwater flow has a negative impact on the artificial freezing project, especially when the salt content of local water is high; it will change the thermal property, which is not conducive to the formation of the frozen wall. Zhao et al. [25] analyzed the influencing factors of the freezing temperature field through three-dimensional finite element analysis software, and gave the suggested values for the saltwater temperature, freezing pipe diameter, and freezing pipe spacing. Zhao et al. [26] combined existing engineering examples and numerical simulation and found that the hydration heat of the cement can hinder the freezing of the soil. Bai et al. [27,28] established a numerical model and carried out a one-side freezing test to find that the freezing of soil is a coupled thermo-hydro-mechanical process.

The influence of external factors on soil temperature has been studied in depth, but very few studies have focused on the effect of the latent heat of the phase change on temperature. The latent heat of the phase change makes it more challenging to judge the soil's state, considering that AGF is fundamentally a phase change process in which water in the soil freezes into ice. This paper explores the spatial and temporal variation in the soil temperature by establishing a soil physical state analysis model. The model was validated through an indoor test on the AGF of a subway cross passage by selecting Hangzhou muddy silty clay as the test soil. The research results provide some guidance for the judgment of the soil state during the AGF of subway cross passages.

2. State of Soil during Freezing and Thawing Period

2.1. Gilpin Soil State Analysis Model

Gilpin [29] analyzed the thermodynamic characteristics of the free water in the soil, simplified the three-dimensional heat transfer problem, regarded soil as a continuous uniform medium, and established an analysis model of the soil state based on the following three basic assumptions. The soil is divided into the frozen zone, unfrozen zone, and frozen fringe, and the temperature field in these zones is linearly distributed. Compared with the latent heat of water, the sensible heat of soil is ignored. The phase change mainly occurs on the bottom of the ice lens and the freezing front, ignoring the heat change caused by the change in unfrozen water in the content in the frozen fringe, as shown in Figure 1.

In Figure 1, V_H , V_a , and V_x are the flow velocities of water seepage in the frozen zone, frozen fringe, and unfrozen zone, respectively; T_1 is the temperature at the interface between the frozen zone and the cooling source, T_2 is the temperature at the ice lens bottom, T_3 is the temperature of the freezing front, and T_4 is the boundary temperature of the unfrozen area; K_1 , K_2 , and K_3 are the slopes of the curves in the frozen zone, frozen fringe and unfrozen zone, respectively.

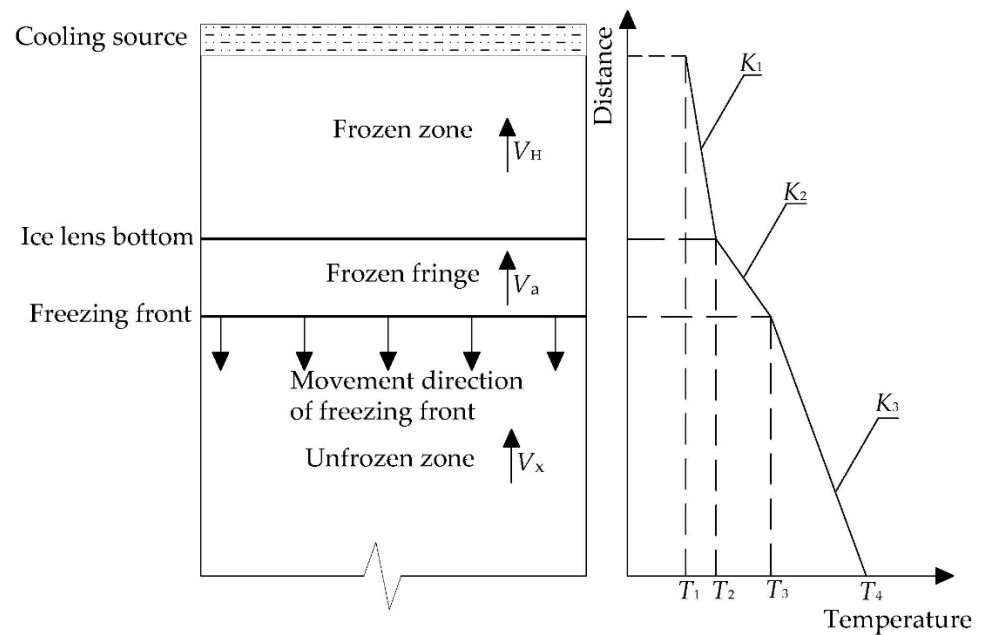


Figure 1. Gilpin soil state analysis model.

Figure 1 shows the following:

The temperature of the soil gradually increases outward from the cooling source. Due to the different state and thermal conductivity of the soil in different zones, the variation rules of temperature and distance are different; that is, the slope of the temperature field curve of the soil is different. After the free water in the frozen fringe is frozen, the water content decreases, which causes the free water in the unfrozen zone to migrate to the frozen fringe under the action of capillaries, forming the water seepage direction shown in Figure 1. The soil freezing causes the porosity of the frozen zone and the frozen fringe to change, which makes the seepage velocity of each zone different. Under the action of freezing and water migration, the frozen fringe continues to move outward, and the frozen zone continues to expand.

2.2. Analysis Model of Soil Physical State in Freezing and Thawing Periods

The Gilpin model ignores the mutation in the soil temperature during freezing and thawing caused by the latent heat of the phase change at the ice–water interface. At the same time, film water migrates to the freezing front and forms discontinuous segregation ice, which makes the frozen ice–water interface irregular and discontinuous [30]. In the process of a frozen fringe movement, the ice–water interface will move repeatedly, and the soil temperature will oscillate and mutate. Based on the Gilpin model, an analysis model of the soil physical state in the freezing and thawing periods was established by comprehensively considering the influence of latent heat on soil temperature, the irregularity of the ice–water interface, and the segregation ice in the frozen fringe. The basic assumptions of the model are as follows:

The soil during the construction process of AGF can be divided into three zones: frozen zone, unfrozen zone, and frozen fringe. The interface between the frozen fringe and the frozen zone is the ice–water interface, and the interface between the frozen fringe and the unfrozen zone is the freezing front. The temperature field in each zone presents a linear distribution. The ice–water interface is not a solid unit, and latent heat cannot be consumed or absorbed by the interface. There is a space entity with a certain thickness bearing latent heat; that is, the influence range of the latent heat is the width of the frozen fringe. Ignoring the thickness change in the frozen fringe during the development process, the influence range of latent heat remains unchanged. The frozen fringe has two layers: the side near the ice–water interface is the segregation ice layer, where the free water is in the mixed state of

ice water, that is, the segregation ice and liquid water (the interface between the two also forms the ice–water interface); the side near the freezing front is the liquid water layer, and the free water is liquid in this layer. The free water phase change occurs instantaneously at the ice–water interface and generates latent heat. The direction of the latent heat transfer is the same as that of the temperature path. Compared with the latent heat of the water, the sensible heat of the soil is ignored.

In Figure 2, the freezing front is the energy field interface, which can penetrate the soil particles and is the farthest distance affected by the latent heat, which is obtained from the connection deviation of the ice–water interface at the farthest end. The one-dimensional temperature field distribution curves of the soil at different times when the latent heat of the phase change and segregation ice are ignored are shown in Figure 3.

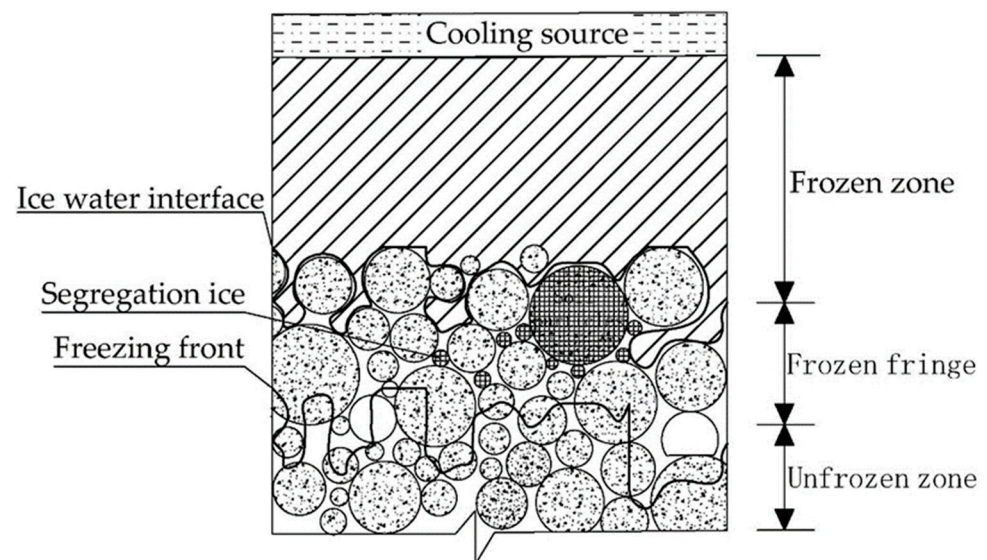


Figure 2. Schematic diagram of the model.

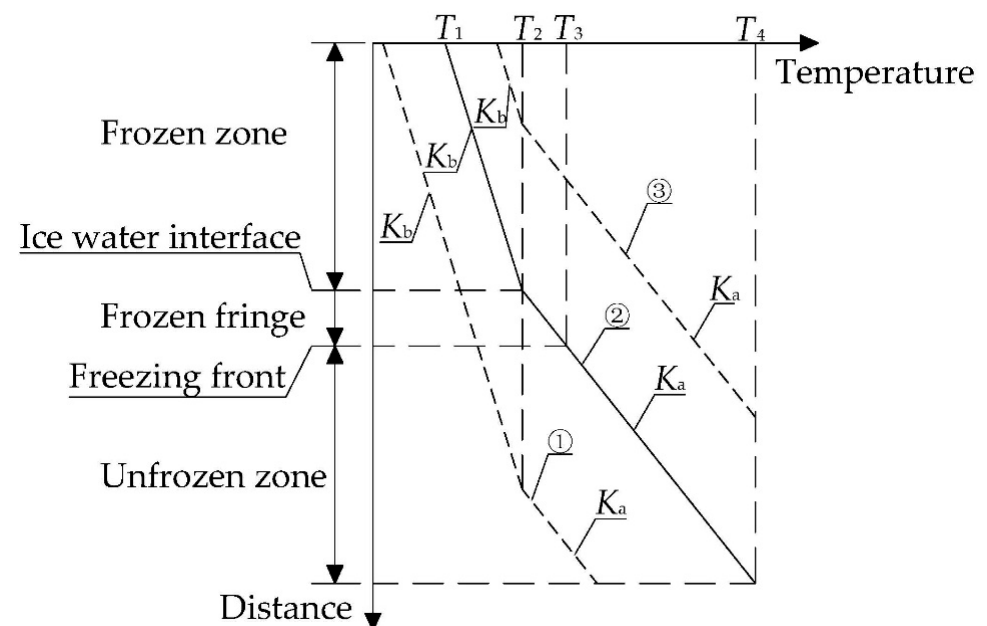


Figure 3. The one-dimensional temperature field distribution curves of soil at different times.

In Figure 3, lines ①, ②, and ③ represent the one-dimensional temperature field distribution curves of the soil at different times; T_1 , T_2 , T_3 , and T_4 , respectively, are the

interface temperature between the frozen zone and cooling source, ice–water interface temperature, freezing front temperature, and the unfrozen zone boundary temperature at the time represented by line ②; K_a , and K_b , respectively, represent the slopes of curves in the frozen zone and unfrozen zone. The thermal conductivity of the frozen zone is different from that of the unfrozen zone, and thus the slope of the curve changes at the ice–water interface. The thickness of the frozen fringe is unchanged, so the temperature of the freezing front does not change. In addition, the freezing temperature of the soil is the same. Therefore, lines ① and ③ in Figure 3 can be obtained by longitudinal translation of line ②.

During the freezing period, the frozen fringe develops from the frozen zone to the unfrozen zone, the curve moves in the order of ③→②→①, and the soil temperature generally decreases. During the thawing period, the frozen fringe retracts from the unfrozen zone to the frozen zone, the curve moves in the order of ①→②→③, and the soil temperature shows an increasing trend.

The phase change and migration of the free water in the soil are the main causes of the frozen fringe movement. In addition, the latent heat is released or absorbed during the phase change, which leads to mutations in the soil temperature. Therefore, on the basis of Figure 3, considering the influence of the latent heat, the one-dimensional temperature field distribution curve of line ② can be obtained, as shown in Figure 4.

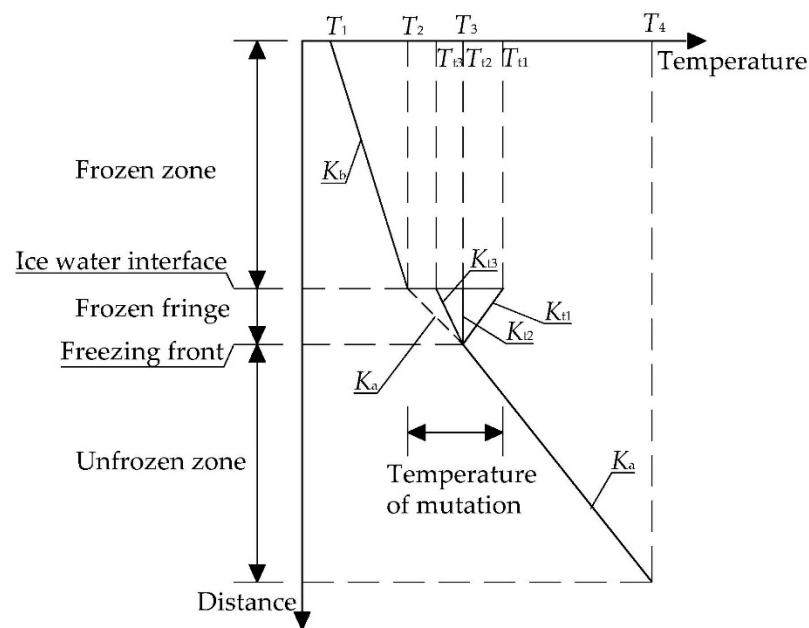


Figure 4. One-dimensional temperature field distribution curve of line ②.

In Figure 4, the temperature of the soil at the ice–water interface mutates due to the influence of the latent heat. Since the influence range of the latent heat is the frozen fringe, the temperature at the freezing front remains unchanged. The temperature of mutation ($T_{ti} - T_2$, $i = 1, 2, 3$) of different soils is different. Therefore, there are three change modes of the soil temperature in the frozen fringe: rising, falling, or unchanged, and the corresponding slope of the curve is K_{ti} ($i = 1, 2, 3$).

The thermal conductivity κ is the heat passing through the soil in a unit area in a unit of time under a unit temperature gradient. The thermal conductivity of the soil is a quantitative expression of the thermal capacity of the soil.

It can be expressed by Fourier's law as follows:

$$Q = -\kappa \frac{dT}{dx} A \quad (1)$$

where Q is heat; κ is the thermal conductivity; A is the heat transfer area; and T is the temperature.

According to Equation (1), when the thermal conductivity κ and heat transfer area A are constant, the soil temperature is determined by the heat Q . The heat in the soil is mainly affected by the external heating source, the cooling source, and the latent heat of the phase change. Assuming the heat provided by the external heating source and the cooling source is Q_{ex} , the total heat causing soil temperature change is Q_t , and the heat of the phase change in the free water in the soil is Q_p .

$$Q_t = Q_{ex} + Q_p \quad (2)$$

According to the one-dimensional temperature field distribution curve of soil, the temperature field state during freezing and thawing is analyzed.

(1) During freezing, the cooling capacity diffuses outward from the cooling source, and the temperature of the soil decreases accordingly. The temperature path is shown in Figure 5.

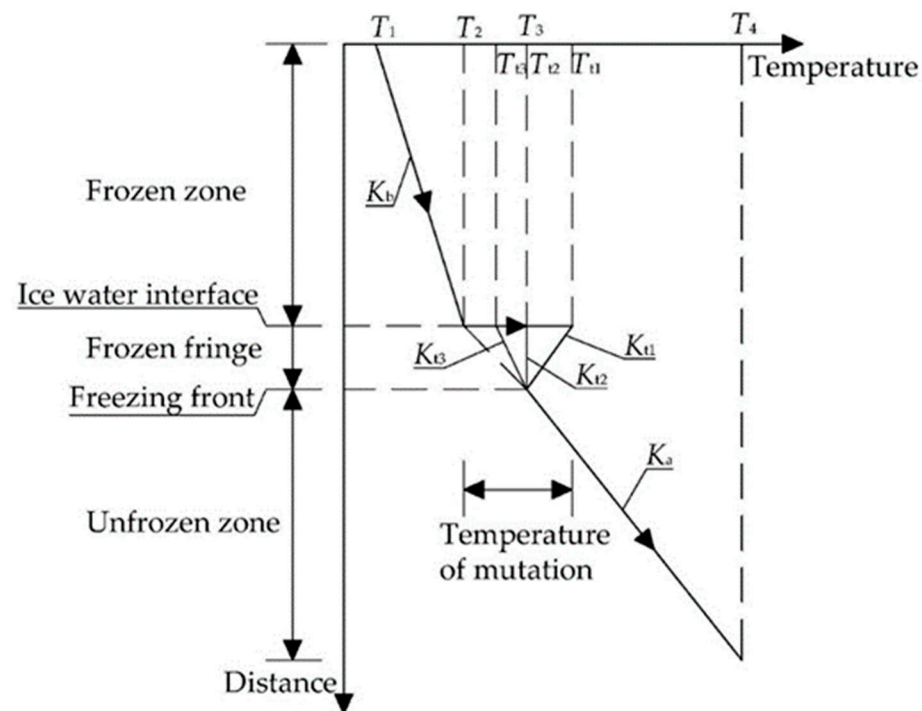


Figure 5. One-dimensional temperature field path during freezing.

In Figure 5, the temperature of the soil shows an overall upward trend from the cooling source to the outside. At the ice–water interface, the free water solidifies and exotherms, and the temperature mutates. The soil in the frozen fringe absorbs latent heat and heats up, and the direction of the latent heat transfer is the same as the direction of the temperature path.

The frozen and unfrozen zones are not affected by the latent heat, $Q_p = 0$, $Q_t = Q_{ex}$. During the freezing period, $Q_{ex} < 0$, and the absolute value of the external heat from the self-cooling source gradually decreases until it reaches 0. Therefore, the temperature of soil increases gradually in the frozen and unfrozen zones. In the frozen fringe, the soil is affected by the latent heat, and $Q_p > 0$. Therefore, the soil temperature of mutation increase on the original basis. The closer the soil is to the ice–water interface, the more obvious the effect of the latent heat, and the greater the temperature of mutation.

(2) During thawing, the cooling source no longer provides cooling capacity. Assuming that the interface between the frozen zone and the cooling source is a completely insulated interface and no heat transfer occurs, the heat of the soil thawing comes from the normal

temperature soil in the unfrozen zone. Under the action of the temperature gradient, the heat diffuses from the unfrozen zone to the frozen zone. The temperature path is shown in Figure 6.

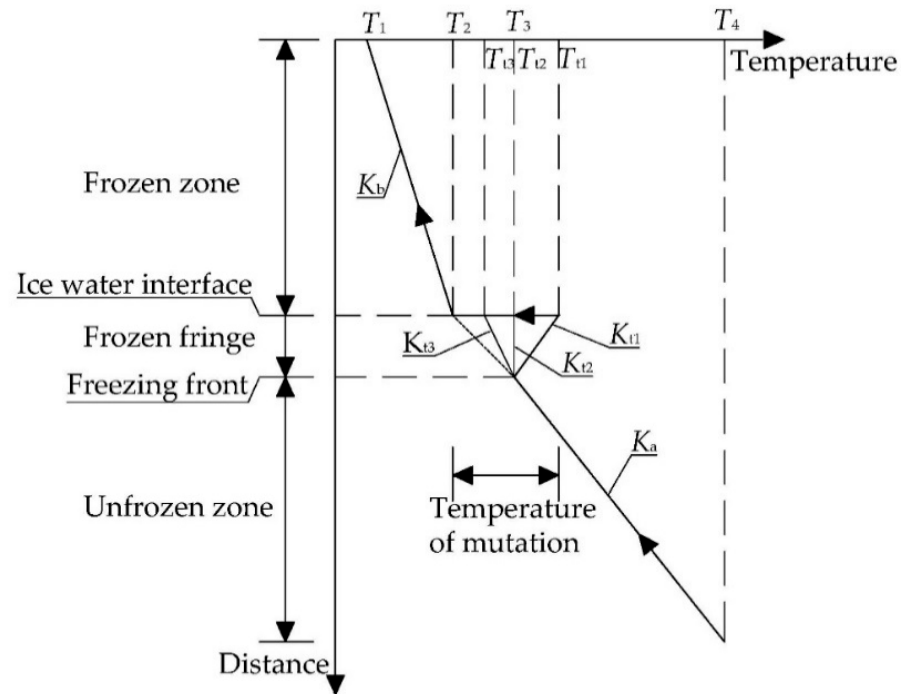


Figure 6. One-dimensional temperature field path during thawing.

As shown in Figure 6, the temperature of the soil gradually decreases from the boundary of the unfrozen zone to the frozen zone. The frozen fringe acts as an endothermic carrier, absorbing heat from the outside and transferring it to the ice–water interface. When the ice melts and absorbs the heat, the soil temperature mutative decreases, and the direction of latent heat transfer is the same as that of the temperature path.

The frozen and unfrozen zones are not affected by the latent heat, $Q_p = 0$, $Q_t = Q_{ex}$. During the thawing period, $Q_{ex} > 0$, gradually decreasing from the unfrozen zone to the frozen zone. Therefore, the temperature in the frozen and unfrozen zones gradually decreases. When $Q_p > 0$, the soil temperature mutation increases compared with that of the original path. The closer the soil is to the ice–water interface, the larger the value of Q_p , and the larger the temperature mutation generated. At the ice–water interface, Q_p reaches its peak, and the temperature mutation value reaches its maximum, which is eventually absorbed by the ice and transformed into the internal energy of water.

2.3. Development Process of Frozen Fringe and Temporal Variation in Soil Temperature

During the period of freezing and thawing, the temperature of the soil changes dynamically with time, and the zone of the soil constantly changes with the movement of the frozen fringe. However, the temperature of the soil changes differently in each zone. Therefore, the temperature of the soil varies with time in different stages. In this section, based on the one-dimensional temperature field distribution curve, the development process of the frozen fringe and the temporal variation in the soil temperature are studied.

(1) During freezing, the ice–water interface moves to the unfrozen zone, and the frozen zone expands. The development process of the frozen fringe and the interval variation of soil at the temperature probe can be represented by the one-dimensional temperature distribution curve at different times, as shown in Figure 7.

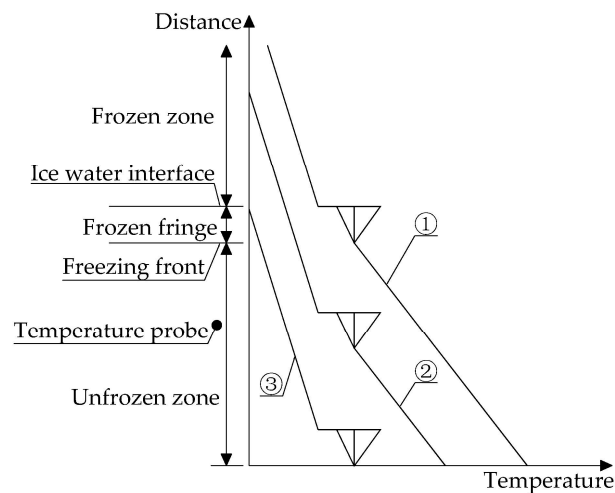


Figure 7. One-dimensional temperature distribution curves at different times during freezing.

In Figure 7, lines ①, ②, and ③ represent the one-dimensional temperature field distribution curves of the soil at different times during the freezing period, developing in the order of ①→②→③. The frozen zone, the frozen fringe, and the unfrozen zone are the divisions of the soil at the time represented by line ①.

The interval variation in the soil at the temperature probe during the freezing period can be divided into the following three stages: soil located in the unfrozen zone (line ①), soil located in the frozen fringe (line ②) and soil located in the frozen zone (line ③). When the soil is located in the unfrozen zone, the probe temperature is the unfrozen zone temperature and gradually decreases with time. When the frozen fringe develops and moves to the location of the probe, the probe temperature is the frozen fringe temperature, which may rise, stay the same, or decrease with time. With the continuous development of the frozen fringe, the ice–water interface passes through the location of the temperature probe, and the temperature mutative decreases. Then, the probe enters the frozen zone, and the probe temperature is the frozen zone temperature, which gradually decreases with time.

The displacement of objects is relative. When the ice–water interface is taken as the reference frame, the soil at the temperature probe moves from the unfrozen zone to the frozen zone during the freezing period, and the movement direction is opposite to the direction of the temperature path in Figure 5. Therefore, the temperature variation curve of the soil with temporal during the freezing period is obtained, as shown in Figure 8.

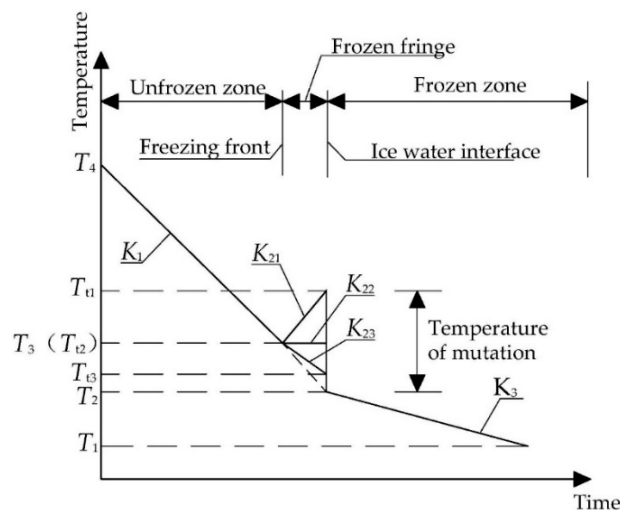


Figure 8. Temperature variation curve of soil with temporal during freezing.

In Figure 8, T_1 , T_2 , T_3 , and T_4 , respectively, represent the interface temperature between the frozen zone and cooling source, the ice–water interface temperature, the freezing front temperature, and the unfrozen zone temperature. $T_{ti} - T_2$, ($i = 1, 2, 3$) is the temperature of mutation; K_1 is the slope of the temperature variation curve with temporal when the soil at the temperature probe is located in the unfrozen zone; K_{21} , K_{22} , and K_{23} , are the slopes of the curves when the soil is located in the frozen fringe; K_3 is the slope of the curve when the soil is located in the frozen zone. The slope of the temperature curve with temporal is different from the slope of the one-dimensional temperature field distribution curve.

(2) During thawing, as the ice in the soil melts and the ice–water interface moves toward the frozen zone, the development process of the frozen fringe and the interval variation in the soil at the temperature probe can be represented by the one-dimensional temperature distribution curve at different times, as shown in Figure 9.

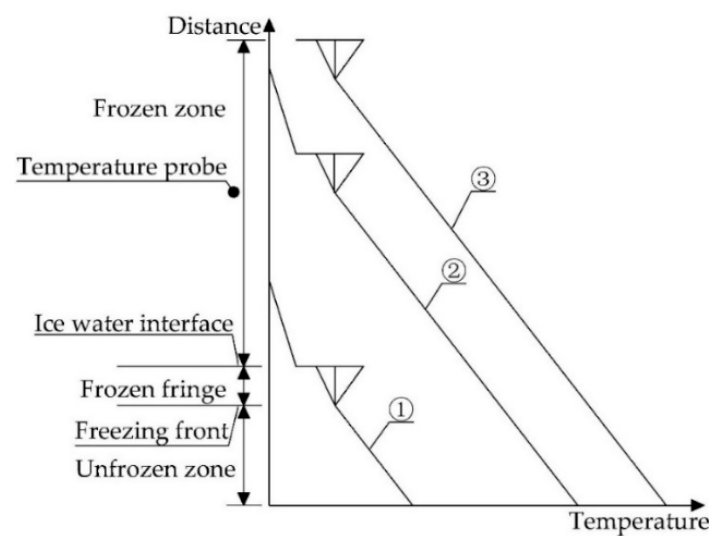


Figure 9. One-dimensional temperature distribution curves at different times during thawing.

In Figure 9, lines ①, ②, and ③ represent the one-dimensional temperature field distribution curves of the soil at different times during the thawing period, developing in the order of ①→②→③. The frozen zone, the frozen fringe, and the unfrozen zone are the divisions of the soil at the time represented by line ①. The interval variation in the soil at the temperature probe during the thawing period can be divided into the following three stages: soil located in the frozen zone (line ③), soil located in the frozen fringe (line ②), and soil located in the unfrozen zone (line ①). When the soil is located in the frozen zone, the probe temperature is frozen temperature and gradually increases with time. When the ice–water interface moves to the location of the probe, the probe temperature is the frozen fringe temperature, which may rise, stay the same, or decrease with time. With the continuous development of the frozen fringe, the probe enters the unfrozen zone, and the probe temperature is the unfrozen zone temperature, which gradually increases with time.

When the ice–water interface is taken as the reference frame, the soil at the temperature probe moves from the unfrozen zone to the frozen zone during the thawing period, and the movement direction is opposite to the direction of the temperature path in Figure 6. Therefore, the temperature variation curve of the soil with temporal during the thawing period is obtained, as shown in Figure 10.

In Figure 10, T_1 , T_2 , T_3 , and T_4 , respectively, represent the frozen zone temperature, ice–water interface temperature, freezing front temperature, and unfrozen zone temperature. $T_{ti} - T_2$, ($i = 1, 2, 3$) is the temperature of mutation; K_1 is the slope of the temperature variation curve with temporal when the soil at the temperature probe is located in the unfrozen zone; K_{21} , K_{22} , and K_{23} are the slopes of the curves when the soil is located in the frozen fringe; K_3 is the slope of the curve when the soil is located in the frozen zone.

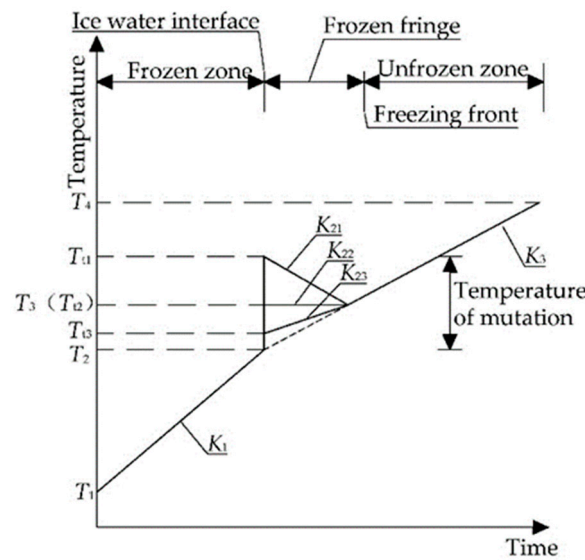


Figure 10. Temperature variation curve of soil with temporal during thawing.

There is not just liquid water in the frozen fringe, but also a lot of discontinuous segregation ice. Therefore, in the movement process of the frozen fringe, the ice–water interface will pass through the soil where the probe is located, resulting in repeated temperature mutations. Finally, the one-dimensional temperature field distribution curve of a certain soil (as shown in Figure 11) and the temperature variation curve of a certain soil with temporal are obtained (as shown in Figure 12).

The temperature of the soil on both sides of the segregation ice layer is different, and the freezing state is also different. Therefore, the freezing and thawing temperatures of the same type of soil are different. As shown in Figures 11 and 12, the freezing index of the soil is T_2 , and the thawing index is T_t . During the freezing period, when the temperature of the probe is lower than the freezing index T_2 , the soil has finished freezing. During the natural thawing period, when the temperature of the probe is higher than the thawing index T_t , the soil has finished thawing.

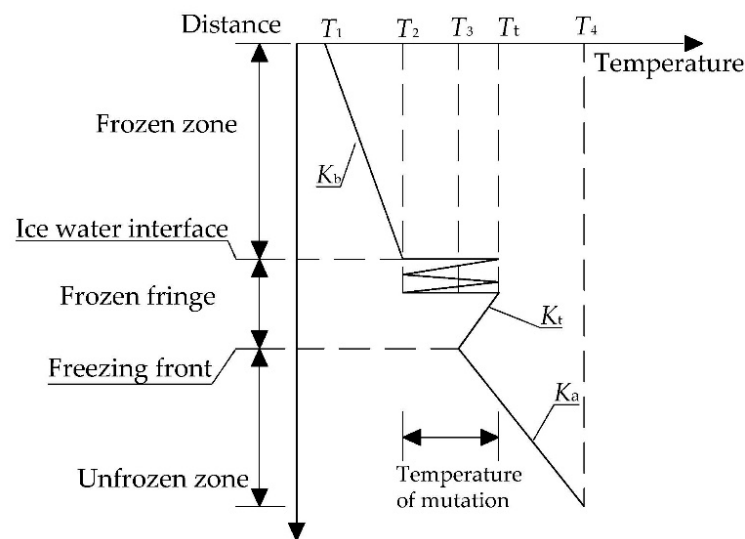


Figure 11. One-dimensional temperature field distribution curve of a certain soil.

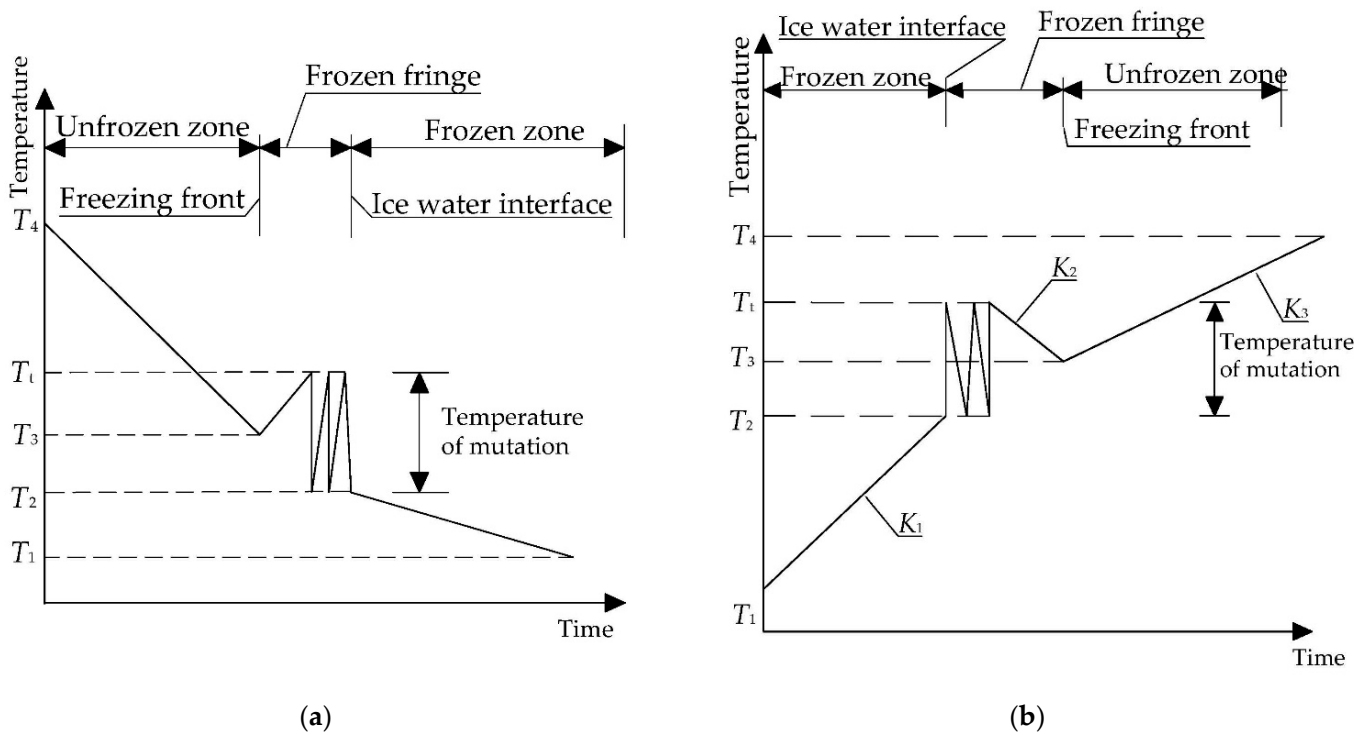


Figure 12. Temperature variation curve of a certain soil with temporal. (a) Freezing curve. (b) Thawing curve.

3. Indoor Model Test

3.1. Test Systems

In order to simulate the temporal and spatial variation in temperature during the freezing and thawing of the frozen soil of a subway cross passage, Hangzhou muddy silty clay located in the typical soft soil area was selected to carry out the indoor model test. The test system is composed of a refrigeration module, a freezing construction simulation module of a subway cross passage, and a temperature measurement module, as shown in Figure 13.

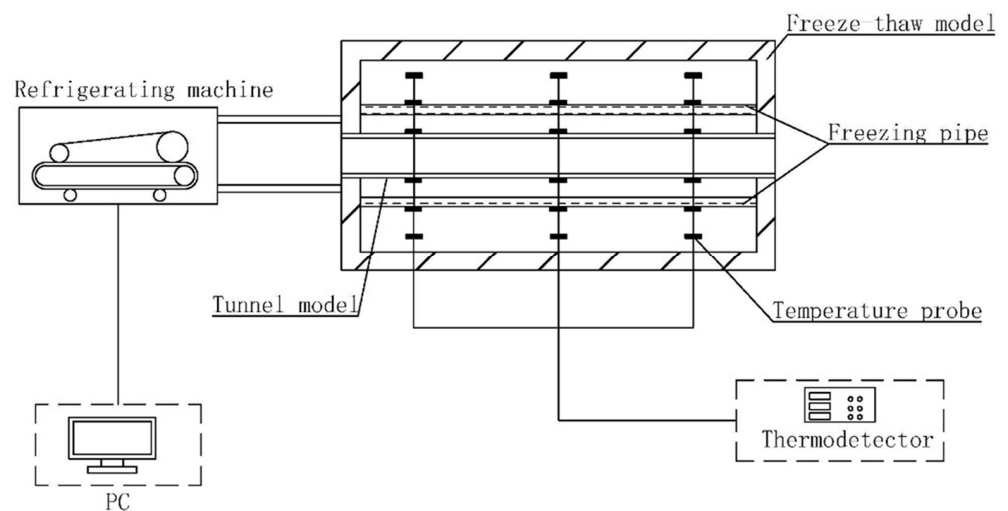


Figure 13. Schematic diagram of test system.

The refrigeration module is composed of a refrigerator, PC, and freezing pipe to provide a cooling source to freeze the soil. The refrigerant is a calcium chloride solution

with the same proportions as those used in the AGF construction project of a subway cross passage. The freezing pipe selected $\Phi 20 \text{ mm} \times 2 \text{ mm}$ copper pipe, prefabricated in the freeze–thaw model, with a total of 8 octagonal arrangements, and a pipe spacing of 100 mm.

The freezing construction simulation module of the subway cross passage is composed of a freeze–thaw model and a tunnel model to simulate the freezing and thawing process of the soil in the freezing construction of subway cross passage.

The outer diameter of the freeze–thaw model is $1000 \text{ mm} \times 1000 \text{ mm} \times 1000 \text{ mm}$, the wall thickness of the model is 51.5 mm, it is made of stainless steel hollow plate, the plate is filled with foam as insulation sandwich, and the bottom thickness of the model is 40 mm; it is made of solid steel plate.

The tunnel model size is determined according to the principle of geometric similarity. The prototype of this model test is a subway tunnel in Hangzhou, whose outer diameter is 6.2 m, inner diameter is 5.5 m, and segment thickness is 0.35 m. The size relationship between the model and prototype is shown in Equation (3).

$$\frac{6.2}{D} = \frac{5.5}{d} = \frac{0.35}{a} = C \quad (3)$$

where D is the outer diameter of the model, d is the inner diameter of the model, a is the wall thickness of the model, and C is the similarity constant.

The maximum outer diameter of the freeze–thaw model that can accommodate the tunnel is 10 mm; therefore, D is 10 mm, the similarity constant C is 62, the inner diameter of the model d is 9 mm, and the thickness of the model tube a is 5 mm.

The temperature measurement module is composed of a temperature probe and thermometer to measure and record the soil temperature at different positions at different times. The temperature probe is buried at different positions in the soil to measure the soil temperature of the point to be measured, and the temperature data are read and recorded by the thermometer.

3.2. Test Scheme

A total of 20 temperature probes were buried at different locations in the soil to monitor the temperature changes during freezing and thawing. The longitudinal section design of this test is shown in Figure 14a. For the convenience of the results analysis and text description, the test system was divided into two sections, A and B, along the longitudinal direction, and each section was divided into two axes and five rings, as shown in Figure 14b,c.

The temperature recording interval of the thermodetector was set to 1 min, and the cooling temperature of the refrigerating machine was set to $-18 \text{ }^\circ\text{C}$. During the test, the temperature of the soil was monitored in real time. When the temperature of all the probes reached a stable state, the refrigerating machine was closed to allow the soil to thaw naturally.

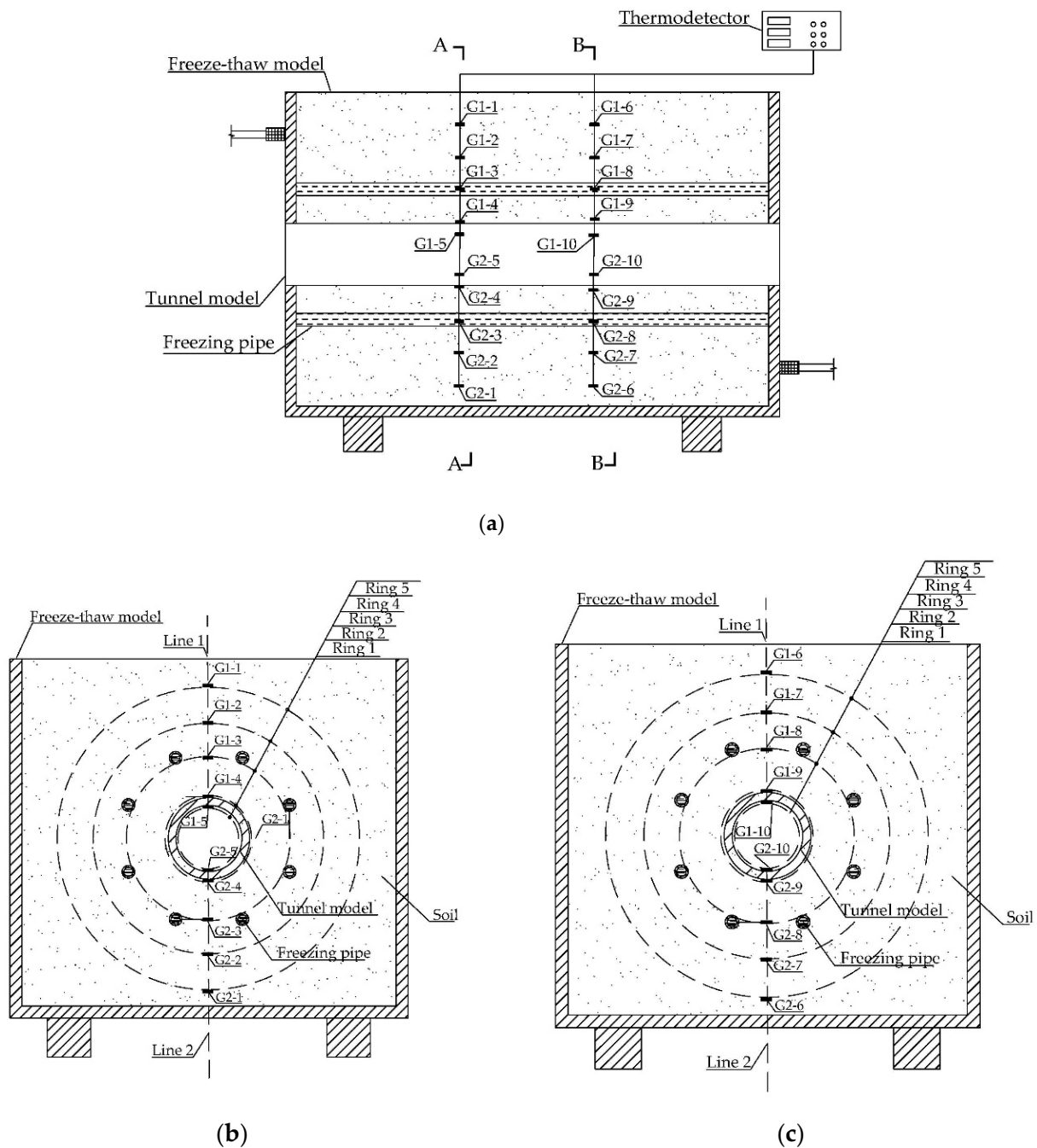


Figure 14. Test section design drawing. (a) Longitudinal section; (b) A-A cross-sectional section; (c) B-B cross-sectional section.

4. Indoor Test Results and Discussion

4.1. Temporal and Spatial Variation in Soil Temperature during Freezing Period

The temporal variation law of the soil temperature was analyzed using the variation curve of the temperature at the temperature probe with temporal. The spatial variation law of the soil temperature was analyzed by controlling all aspects of the frozen soil curtain, and the distance from the temperature probe to the central ring of the freezing pipe was used as the independent variable. There are five different distance levels. Among them, ring 1 is inside the central ring, 90 mm away from the central ring, and the probe is located on the inner wall of the tunnel model. Ring 2 is inside the central ring, 85 mm away from the central ring, and the probe is located on the outer wall of the tunnel. Ring 3 is the

central ring, and the probe is located at the midpoint of the two adjacent freezing pipes. Ring 4 is on the outside of the central ring, 85 mm away from the central ring, and the probe is located in the soil. Ring 5 is on the outside of the central ring, 170 mm away from the center ring, and the probe is located in the soil. The temperature variation curves of the probes with temporal during the freezing period are shown in Figure 15.

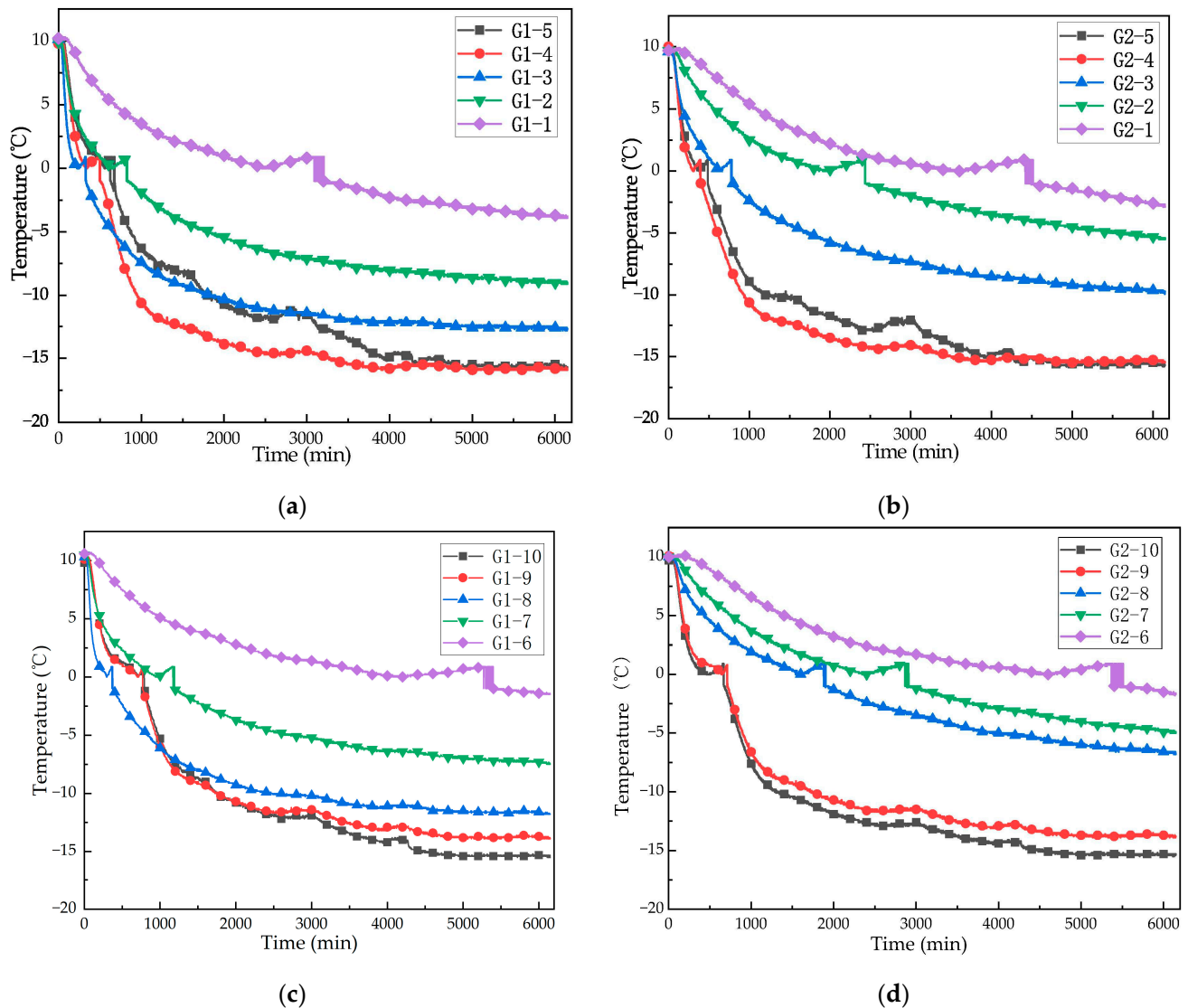


Figure 15. Temperature variation curves of the probes with temporal during the freezing period. (a) Section A, line 1; (b) section A, line 2; (c) section B, line 1; (d) section B, line 2.

(1) The temporal variation law of the soil temperature during freezing

In this test, a total of 20 groups of temperature variation curves with temporal were obtained. The curves were basically the same and showed a downward trend; that is, the soil temperature gradually decreased with time. The initial temperature was 10 °C; when the temperature decreased to 0 °C, it increased; then, when it increased to 0.9 °C, the temperature mutative decreased to −1 °C; following this, the temperature mutated repeatedly between −1 and 0.9 °C; then, it continued to decrease from −1 °C and tended to be stable. According to the test results, the temperature variation curves of the Hangzhou muddy silty clay during freezing are shown in Figure 16.

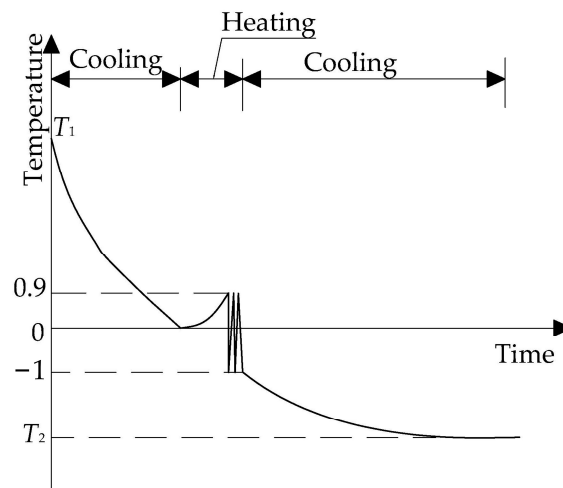


Figure 16. Temperature variation curves of the Hangzhou muddy silty clay during constant temperature freezing.

In Figure 16, the cooling of the unfrozen zone, the heating of the phase transition, and the cooling of the frozen zone are the three stages of soil temperature change during the freezing period. T_1 is the initial temperature before the soil freezes, and T_2 is the stable temperature when the soil temperature reaches a stable state. This conforms to the K_1 - K_{21} - K_3 curve in Figure 8.

The temperature of the soil at the probe showed a repeated mutation phenomenon in the range of $-1\sim 0.9$ °C, which is consistent with the analysis results in Figure 12. In addition, it can be seen that the temperature on the frozen soil side of the ice–water interface of the Hangzhou muddy silty clay was -1 °C, the temperature on the unfrozen soil side was 0.9 °C, and the temperature of mutation was 1.9 °C. Combined with Figure 12, the soil was completely frozen when the probe temperature was lower than -1 °C. This temperature can be used as the freezing index of Hangzhou muddy silty clay.

(2) One-dimensional temperature field distribution of soil during freezing

The temperature curves of rings 1, 2, and 3 with temporal basically coincide before the temperature reaches -1 °C. Then, the temperature of ring 3 is basically higher than that of rings 1 and 2, and the temperatures of rings 1 and 2 are basically the same. The temperature of ring 4 is always higher than that of ring 3, and the temperature of ring 5 is always higher than that of ring 4.

The soil temperature at different distances from the freezing center at different stages is different, and there is an obvious temperature gradient in the one-dimensional temperature field [31]. This phenomenon is explained in combination with Figure 14.

In Figure 14, the freezing center is the center of the central ring (coinciding with the center of the tunnel model). R_1 , R_2 , R_3 , R_4 , and R_5 are the radii of rings 1, 2, 3, 4, and 5, respectively, i.e., the distance between the temperature probe and the freezing center. Ring 3 is the central ring, whose radius is the distance between the center of the freezing pipe and the freezing center. The freezing pipe is divided into inner and outer parts by the central ring. The cold capacity of the inner and outer sides of the freezing pipe is the same, but the soil area of the two sides is different. Taking rings 2 and 4 as an example, the distance between the two rings and the central ring is 85 mm. Since the cold capacity Q is the same, the cold capacity of the soil of rings 2 and 4 per unit area is as follows:

$$q_2 = \frac{Q}{2\pi R_2 dx} \quad (4)$$

$$q_4 = \frac{Q}{2\pi R_4 dx} \quad (5)$$

where q_2 is the per unit area cooling capacity of the soil of ring 2, and q_4 is the per unit area cooling capacity of the soil of ring 4.

From $R_2 < R_4$, as in Equations (4) and (5), it is known that $q_2 > q_4$. Therefore, during the freezing period, the temperature of ring 2 is always lower than that of ring 4. Similarly, it is known that $q_1 \approx q_2 > q_4 > q_5$. The temperature of ring 3 is basically the same as that of rings 1 and 2 before freezing, indicating that $q_1 \approx q_2 \approx q_3$ before freezing.

In summary, the soil temperature starts from the central ring and gradually increases to the boundary of both the inner and outer sides. The test results are consistent with the analytical results in Figure 5. On the same side of the central ring, the farther away from the central ring, the higher the temperature of the soil, and the higher the freezing stability temperature. The effect of distance on the temperature of the soil is, in essence, that the distance changes the cooling capacity of the soil per unit area, and the reason for the difference in the temperature of the soil at the same distance on both sides is the difference in the cooling capacity of the soil per unit area. Therefore, during the freezing period, the cooling laws of soil at the same distance inside and outside the central ring are different. The actual temperature of a certain point in the soil is related to the cooling capacity of the soil per unit volume. The greater the cooling capacity, the lower the soil temperature [3].

4.2. Temporal and Spatial Variation of Soil Temperature during Freezing Period

(1) The temperature variation curves of the probes with temporal during the thawing period are shown below.

As shown in Figure 17, the temperature variation curves of each temperature probe with temporal during thawing are basically the same and showed an upward trend; that is, the soil temperature gradually decreased with temporal. When the temperature reached $-1\text{ }^\circ\text{C}$, the temperature mutative increased to $0.9\text{ }^\circ\text{C}$, then, the temperature mutated repeatedly between -1 and $0.9\text{ }^\circ\text{C}$; following this, it slowly decreased from $0.9\text{ }^\circ\text{C}$ to $0\text{ }^\circ\text{C}$ and continued to decrease until the stable temperature during thawing was about $10\text{ }^\circ\text{C}$. According to the test results, the temperature variation curves of the Hangzhou muddy silty clay during natural thawing are shown in Figure 18.

The temperature of the soil at the probe showed a repeated mutation phenomenon in the range of $-1\sim 0.9\text{ }^\circ\text{C}$, which is consistent with the analysis results in Figure 12. In addition, during the thawing period, the temperature on the frozen soil side of the ice–water interface of the Hangzhou muddy silty clay was $-1\text{ }^\circ\text{C}$, the temperature on the unfrozen soil side was $0.9\text{ }^\circ\text{C}$, and the temperature of mutation was $1.9\text{ }^\circ\text{C}$. Combined with Figure 12, the soil was completely thawed when the probe temperature was higher than $0.9\text{ }^\circ\text{C}$. This temperature can be used as the thawing index of Hangzhou muddy silty clay.

(2) One-dimensional temperature field distribution of soil during freezing

Before the soil temperature reached $0.9\text{ }^\circ\text{C}$, the temperature relationship between each ring temperature probe was $T_{ring5} > T_{ring4} > T_{ring3} > T_{ring2} \approx T_{ring1}$. The soil temperature closest to the freezing pipe increases to a positive value [32].

The one-dimensional temperature field at the air interface shows an obvious temperature gradient before and after thawing. The closer it is to the freezing center, the lower the soil temperature; the closer it is to the air interface, the higher the soil temperature. The distribution state of the temperature field is similar to that in Figure 6. The one-dimensional temperature field distribution state of the box wall interface before thawing is similar to that of the air interface, with an obvious temperature gradient. After thawing, the temperature gradient of each ring is no longer obvious.

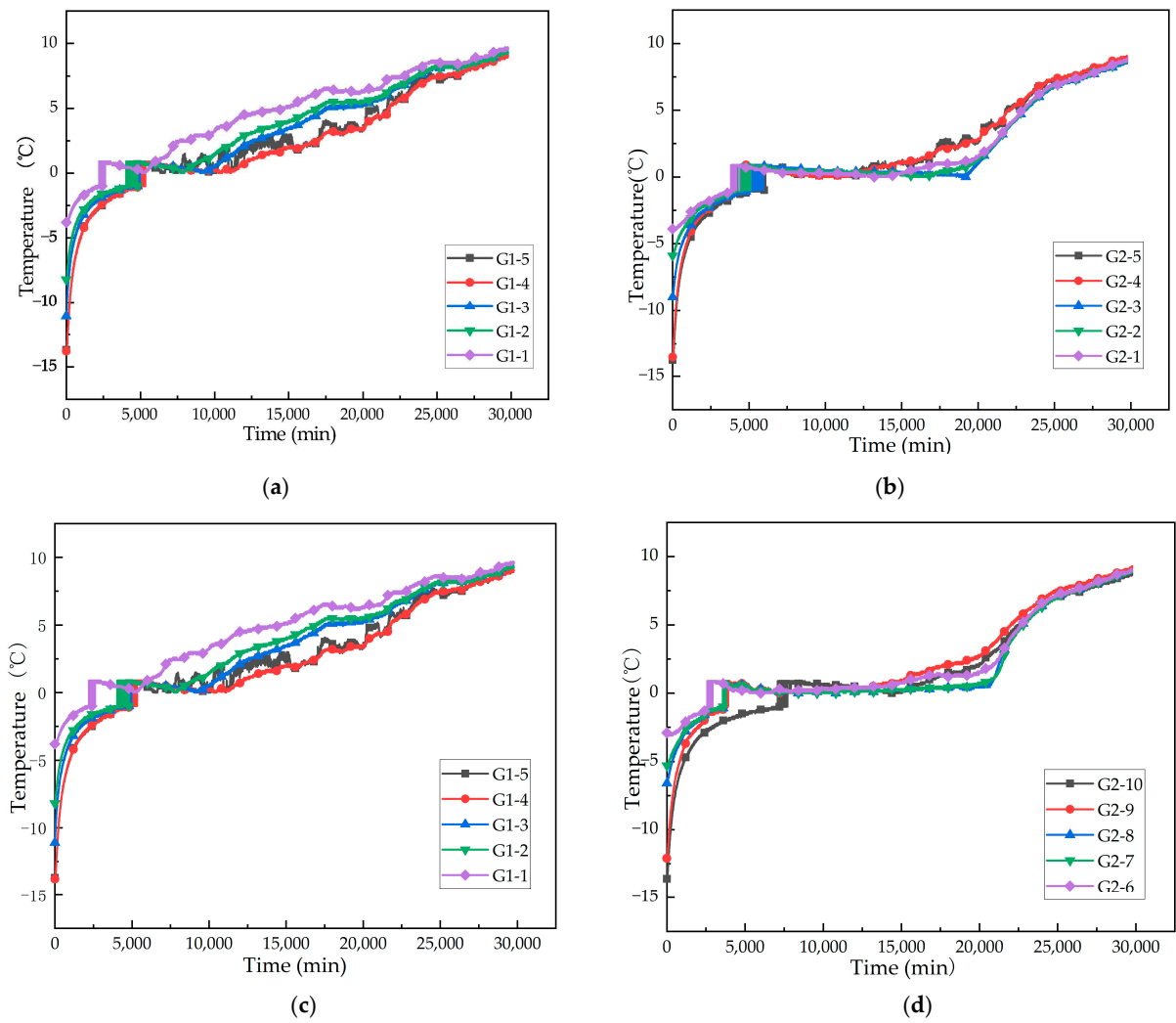


Figure 17. Temperature variation curves of the probes with temporal during the thawing period. (a) Section A, line 1; (b) section A, line 2; (c) section B, line 1; (d) section B, line 2.

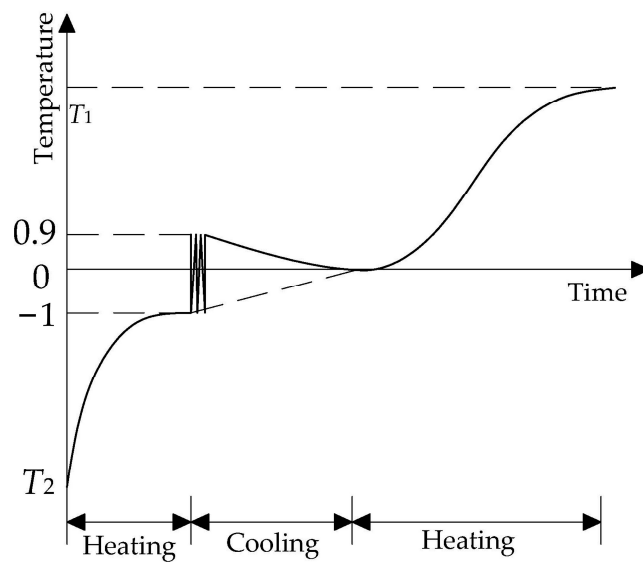


Figure 18. Temperature variation curves of the Hangzhou muddy silty clay during natural thawing.

5. Conclusions

In this paper, the soil temperature variation during the construction of AGF in a subway cross passage was studied using a soil physical state analysis model and an indoor test. The one-dimensional temperature field distribution curve of the soil and temperature variation curve of the soil with temporal were obtained. The results of the indoor test verified the correctness of the model.

1. The temperature is not the same on both sides of the frozen fringe due to the effect of latent heat. It is not appropriate to use the same temperature index to judge whether the soil is frozen or thawed during the construction process. For Hangzhou muddy silty clay, the freezing index is $-1\text{ }^{\circ}\text{C}$, and the thawing index is $0.9\text{ }^{\circ}\text{C}$.

2. During the freezing period, the temperature gradient between the various sectors is obvious. The actual temperature of a certain point in the soil is related to the cooling capacity of the soil per unit volume. During natural thawing, the temperature gradient at the air interface is still obvious, and the thawing time is shorter the closer the soil is to the air. During construction, attention should be paid to the condition of the soil at the interface with the air.

In order to judge the soil freezing state during the AGF of subway cross passages, the sampling interval and layout spacing of temperature probes can be appropriately shortened. According to the physical state analysis model of soil provided in this paper, the frozen soil curtain condition can be analyzed using the temperature variation curve with temporal and the temperature field distribution curve.

Author Contributions: Conceptualization, B.Z.; methodology, X.L.; validation, J.M.; formal analysis, B.K.; investigation, J.M.; resources, J.X.; writing—original draft preparation, B.H. and X.L.; writing—review and editing, B.H. and Q.C.; project administration, B.Z.; funding acquisition, Q.C. and J.X. All authors have read and agreed to the published version of the manuscript.

Funding: The financial support from the National Natural Science Foundation of China (Grant No. 52008373), the Science and Technology Program of Zhejiang Province (Grant No. 2022C35026), the Postgraduate course construction project of Zhejiang University of Science and Technology (Grant No. 2021yjskj05) are greatly acknowledged.

Data Availability Statement: Not applicable.

Acknowledgments: This paper is also supported by the Postgraduate Research and Innovation Foundation of Zhejiang University of Science and Technology.

Conflicts of Interest: The authors declare no conflict of interest.

References

1. Duvarci, Y.; Yigitcanlar, T. Can Tube Tunnel Crossings Relieve Urban Congestion Problems? Izmir Tube Tunnel Project Proposal Under Scrutiny. *Sustainability* **2019**, *11*, 2543. [[CrossRef](#)]
2. Fu, Y.; Hu, J.; Wu, Y.W. Finite element study on temperature field of subway connection aisle construction via artificial ground freezing method. *Cold Reg. Sci. Technol.* **2021**, *189*, 103327. [[CrossRef](#)]
3. Fan, W.H.; Yang, P. Ground temperature characteristics during artificial freezing around a subway cross passage. *Transp. Geotech.* **2019**, *20*, 100250. [[CrossRef](#)]
4. Li, Z.M.; Chen, J.; Sugimoto, M.; Ge, H.Y. Numerical simulation model of artificial ground freezing for tunneling under seepage flow conditions. *Tunn. Undergr. Space Technol.* **2019**, *92*, 103035. [[CrossRef](#)]
5. He, P.P.; Cui, Z.D. Dynamic response of a thawing soil around the tunnel under the vibration load of subway. *Env. Earth Sci.* **2015**, *73*, 2473–2482. [[CrossRef](#)]
6. Rong, C.X.; Wang, B.; Cheng, Y.; Dong, Y.B.; Yang, F. Laboratory model test study on formation mechanisms of artificial frozen walls in permeable strata with high seepage velocity. *Chin. J. Rock Mech. Eng.* **2021**, *41*, 596–613.
7. Yue, F.T.; Zhang, S.B.; Li, W.Y.; Dong, H.B. Study on thaw settlement grouting applied to connected aisle construction with artificial ground freezing method in metro tunnel. *Rock Soil Mech.* **2008**, *29*, 2283–2286.
8. Zhang, D.M.; Xie, X.C.; Zhou, M.L.; Huang, Z.K.; Zhang, D.M. An incident of water and soil gushing in a metro tunnel due to high water pressure in sandy silt. *Eng. Fail. Anal.* **2021**, *121*, 105196. [[CrossRef](#)]
9. Xiao, C.J. Research on the Forming and Thawing of Frozen SOIL Walls by Artificial Ground Freezing Method. Ph.D. Thesis, Tongji University, Shanghai, China, 2007.

10. Hu, J.; Liu, W.B.; Pan, Y.T.; Zeng, H. Site measurement and study of vertical freezing wall temperatures of a large-diameter shield tunnel. *Adv. Civ. Eng.* **2019**, *2019*, 8231458. [[CrossRef](#)]
11. Yue, F.T.; Qiu, P.W.; Yang, G.X.; Shi, R.J. Design and practice of freezing method applied to connected aisle in tunnel under complex conditions. *Rock Soil Mec.* **2006**, *5*, 660–663.
12. Zhang, S.; Yue, Z.R.; Sun, T.; Zhang, J.W.; Huang, B.L. Analytical determination of the soil temperature distribution and freezing front position for linear arrangement of freezing pipes using the undetermined coefficient method. *Cold Reg. Sci. Technol.* **2021**, *185*, 103253. [[CrossRef](#)]
13. Cai, H.B.; Li, S.; Liang, Y.; Yao, Z.S.; Cheng, H. Model test and numerical simulation of frost heave during twin-tunnel construction using artificial ground-freezing technique. *Comput. Geotech.* **2019**, *115*, 103155. [[CrossRef](#)]
14. Wang, T.; Cao, J.Z.; Pei, X.G.; Hong, Z.Q.; Liu, Y.H.; Zhou, G.Q. Research on Spatial Scale of Fluctuation for the Uncertain Thermal Parameters of Artificially Frozen Soil. *Sustainability* **2022**, *14*, 16521. [[CrossRef](#)]
15. Zhan, Z.X.; Cui, Z.D.; Yang, P.; Zhang, T. In situ monitoring of temperature and deformation fields of a tunnel cross passage in Changzhou Metro constructed by AGF. *Arab. J. Geosci.* **2020**, *13*, 310. [[CrossRef](#)]
16. Qiu, P.; Li, P.T.; Hu, J.; Liu, Y. Modeling Seepage Flow and Spatial Variability of Soil Thermal Conductivity during Artificial Ground Freezing for Tunnel Excavation. *Appl. Sci.* **2021**, *11*, 6275. [[CrossRef](#)]
17. Alzoubi, M.A.; Madiseh, A.; Hassani, F.P.; Sasmito, A.P. Heat transfer analysis in artificial ground freezing under high seepage: Validation and heatlines visualization. *Int. J. Sci.* **2019**, *139*, 232–245. [[CrossRef](#)]
18. Gao, X.J.; Li, M.Y.; Zhang, J.W.; Song, J.X. Field research on artificial freezing of subway cross passages in water-rich silty clay layers. *Chin. J. Rock Mech. Eng.* **2021**, *40*, 1267–1276.
19. Qin, B.; Rui, D.H.; Ji, M.C.; Chen, X.Z.; Wang, S.H. Research on influences of groundwater salinity and flow velocity on artificial frozen wall. *Transp. Geotech.* **2022**, *34*, 100739. [[CrossRef](#)]
20. Liu, X.; Shen, Y.P.; Zhang, Z.C.; Liu, Z.J.; Wang, B.L.; Tang, T.X. Field measurement and numerical investigation of artificial ground freezing for the construction of a subway cross passage under groundwater flow. *Transp. Geotech.* **2022**, *37*, 100869. [[CrossRef](#)]
21. Xiang, L.; Wang, F.; Jin, B.C.; Ouyang, A.H. The distribution of temperature field with the construction of connecting passage in red sandstone formation by freezing method. *Chin. Civ. Eng. J.* **2020**, *53*, 306–311.
22. Zhou, J.; Li, Z.Y.; Wan, P.; Tang, Y.Q.; Zhao, W.Q. Effects of seepage in clay-sand composite strata on artificial ground freezing and surrounding engineering environment. *Rock Soil Mech.* **2021**, *43*, 471–480.
23. Xu, P.; Han, S.Q.; Xing, Y. Analysis of Influencing Factors of Temperature Field in Freezing Construction of Metro Connecting Passage. *Geotech. Geol. Eng.* **2022**, *40*, 1331–1343. [[CrossRef](#)]
24. Zhao, Y.X.; Wei, Y.X.; Jiang, J.S.; Jin, H. Effects of Influence Parameters on Freezing Wall Temperature Field in Subway Tunnel. *Sustainability* **2022**, *14*, 12245. [[CrossRef](#)]
25. Fu, Y.; Hu, J.; Liu, J.; Hu, S.B.; Yuan, Y.H.; Zeng, H. Finite element analysis of natural thawing heat transfer of artificial frozen soil in shield-driven tunnelling. *Adv. Civ. Eng.* **2020**, *2020*, 1–18. [[CrossRef](#)]
26. Zhao, J.L.; Yang, P.; Li, L. Investigating influence of metro jet system hydration heat on artificial ground freezing using numerical analysis. *KSCE J. Civ. Eng.* **2021**, *25*, 724–734. [[CrossRef](#)]
27. Bai, R.Q.; Lai, Y.M.; You, Z.M.; Ren, J.G. Simulation of heat–water–mechanics process in a freezing soil under stepwise freezing. *Permafr. Periglac.* **2020**, *31*, 200–212. [[CrossRef](#)]
28. Bai, R.Q.; Lai, Y.M.; Pei, W.S.; You, Z.M. Study on the frost heave behavior of the freezing unsaturated silty clay. *Cold Reg. Sci. Technol.* **2022**, *197*, 103525. [[CrossRef](#)]
29. Gilpin, R.R. A model for the prediction of ice lensing and frost heave in soils. *Water Resour. Res.* **1980**, *16*, 918–930. [[CrossRef](#)]
30. Ming, F.; Li, D.Q.; Huang, X.; Zhang, Y. Study of the ice lens growth during the freezing process. *Chin. Civ. Eng. J.* **2015**, *48*, 346–350.
31. Hu, X.D.; Wu, Y.H.; Li, X.Y. A Field Study on the Freezing Characteristics of Freeze-Sealing Pipe Roof Used in Ultra-Shallow Buried Tunnel. *Appl. Sci.* **2019**, *9*, 1532. [[CrossRef](#)]
32. Zhou, J.; Zhao, W.Q.; Tang, Y.Q. Practical prediction method on thaw deformation of soft clay subject to artificial ground freezing based on elaborate centrifuge modeling experiments. *Tunn. Undergr. Space Technol.* **2022**, *122*, 104352. [[CrossRef](#)]

Disclaimer/Publisher’s Note: The statements, opinions and data contained in all publications are solely those of the individual author(s) and contributor(s) and not of MDPI and/or the editor(s). MDPI and/or the editor(s) disclaim responsibility for any injury to people or property resulting from any ideas, methods, instructions or products referred to in the content.